

Formic acid as a hydrogen source – recent developments and future trends

Martin Grasmann and Gábor Laurenczy*

Received 12th April 2012, Accepted 1st June 2012

DOI: 10.1039/c2ee21928j

Formic acid has recently been suggested as a promising hydrogen storage material. The basic concept is briefly discussed and the recent advances in the development of formic acid dehydrogenation catalysts are shown. Both the state of research for heterogeneous and for homogeneous catalyst systems are reviewed in detail and an outlook on necessary development steps is presented. Formic acid is considered as one of the most promising materials for hydrogen storage today. There are a number of highly active and robust homogeneous catalysts that selectively decompose formic acid to H₂ and CO₂ near to room temperature. Although the activity and selectivity of heterogeneous catalysts have not yet reached the level of homogeneous systems, this gap is closing.

Introduction

The constant growth of earth's population and the rising standards of living are causing a dramatic increase the world's energy consumption. As this rising energy demand is presently met by the ever increasing use of fossil fuels, these resources are dwindling at alarming rates, while the resulting CO₂ emissions lead to global warming with all its environmental and socio-economic consequences. It is clear that to reverse or even attenuate these developments, sustainable and benign energy sources and an efficient way of energy distribution are prerequisites. Various renewable energy sources (*e.g.* wind and solar) have seen large-scale applications over the last decade and capacities are steadily increasing. In terms of energy distribution and storage, hydrogen is considered one of the ultimate energy vectors to connect a decentralized grid of power generators to various end users for

“mobile applications”. Particularly in combination with fuel cell technology, hydrogen has the potential to provide mobile application with an efficient and (locally) emission-free energy source.

When Bockris¹ first envisioned this use of hydrogen as a general energy carrier in 1972, he expected conservatism, the public's fear of hydrogen and a lack of qualified engineering personnel as the main obstacles. Since then it has become clear that one of the major difficulties for the development of a sustainable hydrogen economy is the efficient and safe storage, handling and distribution of its main component, the hydrogen itself. Classical storage technologies, namely pressurization and/or cryogenic liquefaction, suffer from an inherent trade-off between storage density and efficiency.^{2,3} Recently, concepts for the liquid phase storage of hydrogen under ambient conditions using chemical hydrides, *e.g.* borohydrides, hydrazine and especially formic acid, have received considerable attention.⁴⁻⁸

Formic acid (FA) is considered as one of the most promising materials for hydrogen storage today. Even though its

Institut des Sciences et Ingénierie Chimiques, École Polytechnique Fédérale de Lausanne, Lausanne, Switzerland. E-mail: gabor.laurenczy@epfl.ch; Fax: +41 21 69 39780; Tel: +41 21 69 39858

Broader context

In times of dwindling fossil fuel resources and rising concern about anthropogenic global warming, the search for alternative and sustainable energy sources has become more pressing than ever. As the major candidates for renewable energy production (solar and wind) are periodical, storage and delivery are of central interest. It is widely accepted that hydrogen as an energy vector could be a solution for transport/mobile applications, based on its high energy content and the high efficiency with which its chemical energy can be transformed into electricity in state-of-the-art fuel cells. However, due to the extremely low critical point and very low density of hydrogen gas, it is particularly difficult to store efficiently: classical hydrogen storage methods suffer from weight, cost and safety issues. As an alternative, chemical hydrogen storage has found considerable attention and formic acid is among the most promising compounds to achieve it. Formic acid has a high volumetric hydrogen content, favorable physical properties and is simple to use, making it an important aspirant for both mobile and stationary applications. Also, a hydrogen/energy storage-and-release cycle based on formic acid decomposition and carbon dioxide hydrogenation can be envisioned that could solve the inflexibility of decentralized power generation.

low, with the exception of the 100 h⁻¹ at room temperature reported for a platinum phosphine catalyst. During the following years, a number of papers discussed the formic acid decomposition reaction as the unwanted reverse reaction in CO₂ hydrogenation studies: Puddephatt and co-workers observed a TOF of 500 h⁻¹ after 20 min using a dinuclear Ru complex, [Ru₂(μ-CO)(CO)₄(*m*-dppm)₂], without the addition of a base.²⁵ Using a half sandwich Rh(III) complex with a di-hydroxy-substituted bipyridine ligand, [Cp*Rh(bpy)Cl]Cl, (Cp* = pentamethylcyclopentadienyl, bpy = 2,2'-bipyridine) Himeda *et al.* observed a TOF of 238 h⁻¹ at 40 °C.²⁶ A similar catalyst, [Rh^{III}(Cp*)(bpy)H₂O]²⁺ showed some FA decomposition activity at ambient temperature (28 h⁻¹ at 25 °C) in aqueous solution.²⁷ It is interesting to note that a significant pH dependence of the catalyst activity with a pronounced maximum at pH 3.8 was observed, corresponding to the pK_a of formic acid.

The potential of formic acid decomposition as a low-temperature alternative to alcohol reforming as a hydrogen source was demonstrated in 2008 in independent studies, one by our group and one by Beller and co-workers. Beller's group^{28–31} studied an extensive number of different homogeneous catalyst precursors at 40 °C, including RhCl₃·*x*H₂O, [RuCl₂(*p*-cymene)]₂, RuCl₂(PPh₃)₃, [RuCl₃(benzene)₂]₂ and RuBr₃·*x*H₂O, in the presence of different amines and different phosphine ligands (Table 1). The catalytic activity and stability changed significantly with the amine/HCOOH ratio as well as the type and concentration of ligands: bidentate phosphine ligands with short alkyl groups like 1,2-bis(diphenylphosphino)ethane (dppe) gave generally better activity than their equivalents with longer carbon chains (*e.g.* 1,2-bis(diphenylphosphino)butane (dppb)).

Of all the catalyst–ligand–amine combinations examined, RuBr₃·*x*H₂O in a 5HCOOH/2NEt₃ reaction mixture containing an initial equivalent of 3 triphenylphosphine (PPh₃) per Ru showed the best performance, yielding an initial TOF of 3630 h⁻¹ at 40 °C after a 2 h pretreatment in 80 °C DMF. Similar activities (initial TOF of 2688 h⁻¹) were observed using RuCl₂(PPh₃)₃ under identical conditions. Both catalytic systems were shown to decompose formic acid selectively to H₂ and CO₂ with no detectable level of CO as a byproduct. It has to be noted that, due

to the dependence of the catalyst activity on the HCOOH/amine ratio and the batch type nature of the reported experiments, both the reaction conditions and the hydrogen generation rate are far from constant and these TOF values can only give an indication about the catalysts' true performance.

Connecting their reactor to a fuel cell, the authors provided proof that the hydrogen produced under their conditions could be used directly to generate electricity without CO removal. No poisoning of the fuel cell catalyst was observed when all traces of amine vapor had been removed from the hydrogen by means of an activated carbon filter. Using an optimized catalytic system generated *in situ* from dimeric Ru(benzene) dichloride [RuCl₂(benzene)]₂ with *N,N*-dimethyl-*n*-hexylamine and six equiv. of dppe in a setup for continuous hydrogen generation, Beller *et al.* achieved a total TON of 260 000 over a period of two months with an average TOF of 900 h⁻¹.³⁰ They also reported that the decomposition of formic acid over certain Ru based catalysts can be accelerated or even triggered by irradiation with light.³² The effect was shown to depend both on the catalyst precursor and ligand, yielding an activity increase of more than one order of magnitude for an [RuCl₂(benzene)]₂/12PPh₃ catalyst system. The authors suggested the photo-assisted dissociation of η⁶-benzene during the formation of the active catalyst as well as a non-defined photo-assisted regeneration of this active catalyst as potential mechanisms.

At the same time, our group reported the efficient decomposition of formic acid using a water soluble Ru-based catalyst synthesized by combining [Ru(H₂O)₆]²⁺ or commercial RuCl₃·*x*H₂O with two equivalents of *meta*-trisulfonated triphenylphosphine (*m*TPPTS),^{33,34} patented in 2006. The addition of HCOONa to the aqueous formic acid solution (acid to formate ratio 9 : 1) was shown to increase the catalytic activity by a factor of 50. Recycling the catalyst resulted in a further activity increase, which was assigned to the formation of the active catalyst species during the first run. No catalyst deterioration was observed during more than 100 additional recycle runs, yielding full HCOOH conversion at 90 °C. Despite these high reaction temperatures, no CO formation was observed by FTIR (3 ppm detection limit). Once formed, the active catalyst species did not

Table 1 Homogeneous catalysts for the decomposition of formic acid

Catalyst (precursor) and ligands	Solvent/medium	Performance	T/°C	Ref.
[Ru ₂ (<i>m</i> -CO)(CO) ₄ (<i>m</i> -dppm) ₂]	Acetone	TOF = 500 h ⁻¹	RT	25
RuBr ₃ · <i>x</i> H ₂ O, 3 equiv. (PPh ₃) ₃	5HCOOH/2NEt ₃	Init. TOF = 3630 h ⁻¹	40	28
RuCl ₂ (PPh ₃) ₃	5HCOOH/2NEt ₃	Init. TOF = 2688 h ⁻¹	40	31
[RuCl ₂ (benzene)] ₂ 6 equiv. dppe	<i>N,N</i> -dimethyl- <i>n</i> -hexylamine	TOF = 900 h ^{-1a} , TON = 260 000	40	30
RuCl ₃ · <i>x</i> H ₂ O, 2 equiv. TPPTS	Aqueous HCOONa	TOF = 460 h ⁻¹	120	33
RuCl ₃ , 2 equiv. <i>m</i> TPPTS	Aqueous HCOONa	TOF = 476 h ⁻¹	90	35
([Rh ^{III} (Cp*)(H ₂ O)(bpy)] ²⁺)	Aqueous HCOONa	TOF = 28 h ⁻¹	RT	27
[Ir ^{III} (Cp*)(H ₂ O)(bpm)Ru ^{II} (bpy) ₂] ⁴⁺	Aqueous HCOONa	TOF = 426 h ⁻¹	RT	36
([Ir(Cp*)-4,4'-hydroxy-2,2'-bipyridine])	Aqueous	TOF = 3100 h ⁻¹	60	38
		TOF = 1.4 × 10 ⁴ h ⁻¹	90	
[Ru ₂ (HCO ₂) ₂ (CO) ₄]	TEA	TOF = 1.8 × 10 ⁴ h ⁻¹ , 200 ppm CO	120	39
[Ru ₄ (CO) ₁₂ H ₄]	DMF	TOF = 1470 h ⁻¹	107	41
[{RuCl ₂ (<i>p</i> -cymene)} ₂]	IL ([Et ₂ NEMim]Cl)	TOF = 1540 h ⁻¹	80	43
RuCl ₃	IL ([EMMIM][OAc])	TOF = 280 h ⁻¹	80	45
[Fe(BF ₄) ₂].6H ₂ O, 2 equiv. PP ₃	Propylene	TOF = 1942 h ⁻¹	40	51
	Carbonate	TOF = 5390 h ^{-1a}	80	

^a Continuous run.

change its catalytic properties even after various tests at elevated temperatures up to 170 °C, multiple reruns and exposure to air and more than one year in solution. It is interesting to note that the catalytic activity is not influenced by the CO₂ and H₂ pressure even up to 75 MPa or by the dissolved H₂ and CO₂ (products) concentrations and remains stable. This is a highly relevant feature for applications where the produced gas is either stored directly or where the high pressure can be used as the driving force in a downstream H₂ purification step. A detailed kinetic study using multinuclear NMR spectroscopy led us to the proposition of a reaction mechanism consisting of two competitive catalytic cycles with a monohydride ruthenium complex as a common intermediate species. Recently, we investigated the influence of different sulfonato aryl and aryl-/alkylphosphine ligands as well as the Ru concentration on the formic acid decomposition activity using RuCl₃ as the catalyst precursor.³⁵ Ligand basicity, its hydrophilic properties due to the sulfonate group number and position, as well as steric effects were identified as the main parameters for the catalyst activity. Of all the phosphine ligands investigated, *meta*-disulfonated triphenylphosphine (*m*TPPDS) and *meta*-trisulfonated triphenylphosphine (*m*TPPTS) were found to give optimum compromises between these parameters, leading to maximum formic acid decomposition rates. A distinct maximum in catalyst activity (TOF of 476 h⁻¹ at 90 °C) was observed for an Ru^{III} precursor concentration of 28 mmol L⁻¹ using two equivalents of *m*TPPDS. The activity drop with increasing catalyst concentration was explained by the successive formation of less active chloro-bridged dimeric species, as the reaction mixture contains Cl⁻ from the synthesis.

In the wake of the studies by Beller and Laurency, the rising interest in formic acid as a potential hydrogen storage material has resulted in a number of catalyst studies dedicated to the selective decomposition of formic acid: Fukuzumi *et al.* used an Rh^{III} aqua complex with an unsubstituted bipyridine (bpy) ligand ([Rh^{III}(Cp*)(H₂O)(bpy)]²⁺) as the catalyst to decompose FA at 25 °C.²⁷ While the observed catalytic activity was low (a maximum TOF of 28 h⁻¹ at pH 3.8), studying the H/D exchange and deuterium kinetic isotope effects led to the development of a reaction mechanism with the elimination of β-hydride from an Ru formate species as rate determining step. More recently the same group presented a highly efficient heterodinuclear iridium–ruthenium complex, [Ir^{III}(Cp*)(H₂O)(bpm)Ru^{II}(bpy)₂]⁴⁺.³⁶ Relatively high TOF values of up to 426 h⁻¹ were observed in an aqueous HCOOH–HCOONa solution at room temperature and an optimized pH of 3.8, without the formation of CO.

Based on his work on CO₂ hydrogenation,^{26,37} Himeda³⁸ investigated different Ru, Rh and Ir based catalysts with 4,4'-substituted 2,2'-bipyridine ligands for their performance in the decomposition of formic acid in aqueous media. Of those investigated, only the Ir based catalyst with a 4,4'-hydroxy-substituted bipyridine (DHBP) ligand ([Ir(Cp*)(4,4'-hydroxy-2,2'-bipyridine)] and SO₄²⁻ as the anion yielded substantial activity (TOF of 2800 h⁻¹ at 60 °C). Increasing the temperature to 90 °C increased the TOF to a remarkable 1.4 × 10⁴ h⁻¹ without any CO formation or catalyst degradation. Varying the metal center or the bipyridine 2,2'-substituents led to a significant decrease in catalytic activity in all the investigated cases. The author also investigated the effect of formic acid concentration

and pH on the FA decomposition rate at 60 °C. When changing the FA concentration, a pronounced maximum in the catalytic activity is observed for a 4 M formic acid solution (3100 h⁻¹), with a sharp drop towards higher concentrations. Increasing the pH by adding sodium formate to the reaction mixture led to a continuous decrease in the catalyst activity, from a maximum initial TOF of 2500 h⁻¹ observed for pure HCOOH in water to no measurable activity for a pH of 4.5. This strong pH influence is attributed to the acid–base equilibrium of the hydroxyl group on the ligand, tuning the catalyst structure between its pyridinol and pyridinolate form. This effect is also used to explain the high catalyst activity and the strong substituent effect between OH, OMe, Me and H. Recently, Himeda *et al.* investigated the interconversion between formic acid and H₂/CO₂ using the same Rh and Ru bipyridine catalysts from earlier works.⁸⁴ Reasonably high activities were observed for both reactions using the [Ru(Cp*)DHBP] catalyst, while [Rh(Cp*)DHBP] deactivated quickly during the CO₂/bicarbonate hydrogenation under basic conditions. In this context it is interesting to note that for both the Rh and Ru catalysts with the DHBP ligand, the pH dependence of the FA decomposition activity was markedly different from the corresponding Ir catalyst, with a maximum between pH 2.5 and 4 and an activity drop for pure formic acid in water.

Wills and co-workers investigated several Ru^{II} and Ru^{III} catalyst precursors ([Ru₂Cl₂(DMSO)₄], [RuCl₂(NH₃)₆], [RuCl₃] and [Ru₂(HCO₂)₂(CO)₄]) in triethylamine (TEA) at 120 °C, explicitly without the addition of phosphine ligands.³⁹ As can be expected for such high temperatures, FA decomposition activities were found to be exceptionally high (up to *ca.* 1.8 × 10⁴ h⁻¹). Unfortunately, the CO concentration consistently exceeded 200 ppm for all the catalysts tested. The authors suggest the formation of [Ru₂(HCO₂)₂(CO)₄] as the active species common to all the precursors under these reaction conditions. It is interesting to note that during reuse, all the catalysts exhibited a slight activity increase with each run, indicating ongoing formation of the active catalyst species. The same group later used their [Ru₂Cl₂(DMSO)₄]/TEA system in an attempt to continuously decompose formic acid at a rate approaching the catalyst's maximum activity without acid accumulation in the system.⁴⁰ Of the two concepts tested – one temperature based, the other using an impedance probe – the latter gave promising results, even though the gas flow decreased slightly over several days. Still, this report remains the only one today to address the issue of catalyst efficiency in relation to catalyst drowning due to formic acid accumulation.

Last year Olah *et al.* observed a different group of Ru carbonyl complexes whilst investigating the behavior of RuCl₃ in an aqueous formic acid solution.⁴¹ After the addition of NaCOOH, the formation of H₂ and CO₂ was observed at a TOF of 275 h⁻¹ at 100 °C with a considerable amount of CO (0.21%) as the byproduct. A tetranuclear ruthenium complex [Ru₄(CO)₁₂H₄] consisting of a distorted tetrahedral metal core was identified as the active catalyst species, indicating that the Ru species react with CO from FA decarbonylation to form the catalyst. When the reaction was carried out using an HCOOH–NaCOOH mixture in DMF instead of water, the activity increased substantially (TOF of 1470 h⁻¹ at 107 °C). This was explained by the improved solubility of [Ru₄(CO)₁₂H₄]. However, recycling experiments showed a substantial deactivation after the first run.

For all formic acid decomposition processes taking place in a liquid solvent–acid mixture, contamination of the generated hydrogen with CO₂ and traces of solvent vapor greatly complicates their commercial industrial application. High CO₂ contents can cause a dramatically decreased fuel cell efficiency and increase hydrogen losses *via* necessary purge streams. Solvent traces, while not necessarily harmful to the fuel cell catalyst, constitute losses from the reaction mixture and have to be replaced to maintain constant reaction conditions. Also, most of the organic solvents used in the catalyst studies described here are subject to emission regulations and will require an additional off-gas cleaning step. A promising approach to avoid solvent evaporation altogether is based on the use of ionic liquids (ILs) as the reaction medium, as their negligible vapor pressure effectively suppresses product contamination. Defined as organic liquid electrolytes with a melting point below 100 °C they offer the possibility of tuning the polarity, solubility and functionality according to the system requirements. For example, certain ILs exhibit high solubility for CO₂ – a feature highly relevant for the H₂ production from FA, as it could be used as a first step in gas separation, *i.e.* pure H₂ production. In a first attempt, Deng *et al.* tested the activity of a commercial Ru-based catalyst, $[\{\text{RuCl}_2(\textit{p}\text{-cymene})\}_2]$, in a number of amine-group-functionalized ILs.⁴² TOF values up to 627 h⁻¹ at 40 °C were reached for a mixture of *i*Pr₂NEMimCl and HCOONa. However, a percentage of FA equivalent to the amount of IL remained in the reactor and the catalyst was fully deactivated after a first run to maximum FA conversion. Almost at the same time, Scholten and co-workers found that the same catalyst, $[\{\text{RuCl}_2(\textit{p}\text{-cymene})\}_2]$, in $[\text{Et}_2\text{NE-Mim}]\text{Cl}$ was highly active in the decomposition of FA, yielding TOFs of up to 1540 h⁻¹ at 80 °C without the addition of formate.⁴³ Interestingly enough, Deng and co-workers had discarded that particular catalyst–IL combination in their study as non-active. However, no explanation is given for this discrepancy. In a different approach, Nakahara and co-workers suggested the reversible storage of hydrogen as formic acid in 1,3-dipropyl-2-methylimidazolium formate using $(\text{RuCl}_2(\text{PPh}_3)_4)$.⁴⁴ The authors found that due to a stabilizing effect of the IL on dissolved FA, the equilibrium of reaction 1 (Scheme 1) can be shifted down to increase FA concentrations by CO₂ and H₂ pressure alone at temperatures already as low as 40 °C.

Recently, Wasserscheid and co-workers reported the successful decomposition of FA in ILs based on 1-ethyl-3-methylimidazolium ([EMIM] and 1-ethyl-2,3-dimethylimidazolium ([EMMIM]) as cations in combination with various anions, using RuCl₃ as the catalyst precursor.⁴⁵ They found that the catalytic activity and selectivity as well as its stability are strongly influenced by the nature of both the anion and the cation. Results of the initial screening experiments at 80 °C ranged from only 25.8% FA conversion and 70% selectivity towards CO for [EMIM][PF₆] to 91.1% conversion without any CO formation for [EMMIM][OAc] (Fig. 1). During reuse experiments, the latter proved to be not only stable but exhibited an increase in activity to a stable 280 h⁻¹ after three recycles. This activity change was ascribed to an induction period during which the Ru(III) catalyst precursor is reduced to the Ru(II) active catalyst species, as we have already suggested for our catalyst system.

Beller *et al.*^{46,47} in cooperation with our group investigated the feasibility of a formate/bicarbonate cycle as reversible hydrogen

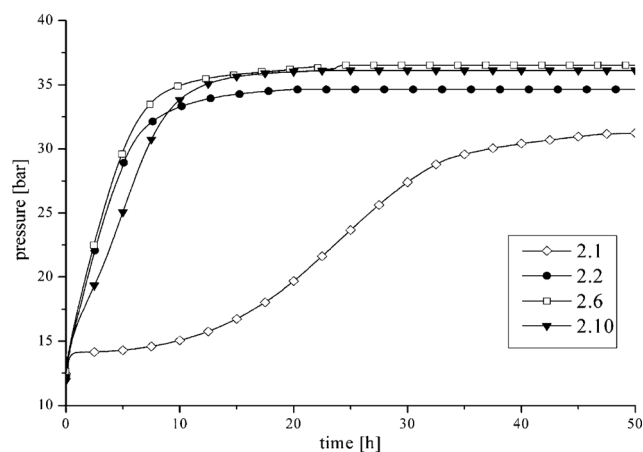


Fig. 1 Pressure/time profiles for the decomposition of formic acid in ionic liquid RuCl₃/[EMMIM][OAc] system as catalyst precursor. Catalyst formation and stabilization during 9 recycling runs (2.1–2.10) at 80 °C. Reproduced from ref. 45 with permission. Copyright Royal Society of Chemistry 2011.

storage system, creating a closed carbon cycle with CO₂ reuse during hydrogen uptake. Both hydrogen release and uptake of various carbonates, bicarbonates and hydroxides with their corresponding formates were investigated using $[\{\text{RuCl}_2(\textit{benzene})\}_2]$ as the catalyst precursor in the presence of 1,2-bis(diphenylphosphino)methane (dppm) in water/DMF (5 : 1). Only the system NaHCO₃/HCOONa was found to give excellent activity and good formate/carbonate yields at moderate temperatures (40–60 °C) and 8 MPa of H₂. In a proof of principle experiment the reuse of the Ru catalyst in a full hydrogenation/decomposition cycle experiment was tested with both NaHCO₃ and HCOONa as the starting material. In both cases the catalyst remained active during the second step but the target product yield dropped considerably.

Taking the concept one step further, Joó and co-workers⁴⁸ in cooperation with our group studied a truly rechargeable hydrogen storage and delivery system based on the carbonate/formate cycle. The equilibrium shift of the reaction $\text{HCOO}^- + \text{H}_2\text{O} = \text{HCO}_3^- + \text{H}_2$ was achieved by repeatedly changing the hydrogen partial pressure between 10 MPa and ambient in a closed reaction vessel containing an aqueous solution of HCO₃Na and $[\{\text{RuCl}(\textit{mTPPMS})_2\}_2]$ (*mTPPMS* = sodium diphenylphosphinobenzene-3-sulfonate). Formate formation and hydrogen uptake at high pressure and carbonate formation under hydrogen release at low pressure were observed using ¹³C NMR analysis to track the molar distribution between formate and bicarbonate species (Fig. 2). The process turned out to be highly selective and fully reversible, albeit relatively slow. The formate decomposition in particular slowed down to around 40–50% conversion, so approximately half the nominal hydrogen storage capacity was accessible.

Recently, Beller and co-workers reported the successful decomposition of formic acid by different Fe based organometallic catalysts when irradiated with visible light.⁴⁹ The initial Fe₃(CO)₁₂ precursor with 6,6'-(phenyl)-2,2':6,2''-terpyridine and PPh₃ as ligands exhibited an initial TOF of 200 h⁻¹ at 60 °C without any CO in the product. However, dissociation of CO

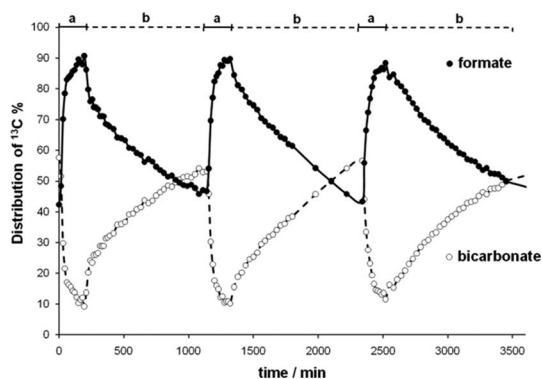


Fig. 2 Hydrogen generation and storage using an aqueous formate/bicarbonate solution: relative amounts of formate and bicarbonate during multiple charge–discharge H_2 pressure cycles. (a) hydrogen storage at 100 bar, (b) hydrogen release at 1 bar. Reproduced from ref. 48 with permission. Copyright Wiley-VCH 2011.

leads to a quick deactivation of the catalytic system. In a follow-up study, the effect of different phosphine ligands was investigated by successively replacing PPh_3 .⁵⁰ Two benzyl-substituted phosphines, benzyl-diphenylphosphine (PPh_2Bn) and tribenzylphosphine (PBn_3) significantly improved the activity (two-fold) and stability (TON of 1266) of the original system. This effect was ascribed to an *ortho*-metalation of the Fe– PBn_3 complex.

Based on this preliminary work, highly active Fe catalysts capable of decomposing formic acid were developed by Beller and our group very recently.⁵¹ A range of organic iron and iron hydride catalyst precursors, including $[Fe(BF_4)_2] \cdot 6H_2O$, $[FeH(PP_3)]BF_4$, $[FeH(H_2)(PP_3)]BF_4$, $[FeH(H_2)(PP_3)]BPh_4$ and $[FeCl(PP_3)]BF_4$, were investigated using tris[2-diphenylphosphino] ethyl]phosphine (PP_3) as the phosphine ligand in propylene carbonate as the solvent (Fig. 3). Except for $[FeCl(PP_3)]BF_4$, excellent activities were observed for all the systems, with a maximum TOF of $1942\ h^{-1}$ after 3 h at $40\ ^\circ C$ using $[Fe(BF_4)_2] \cdot 6H_2O$ with an equivalent of $2PP_3$. Using this catalyst with 4 equiv. of PP_3 in a continuous hydrogen

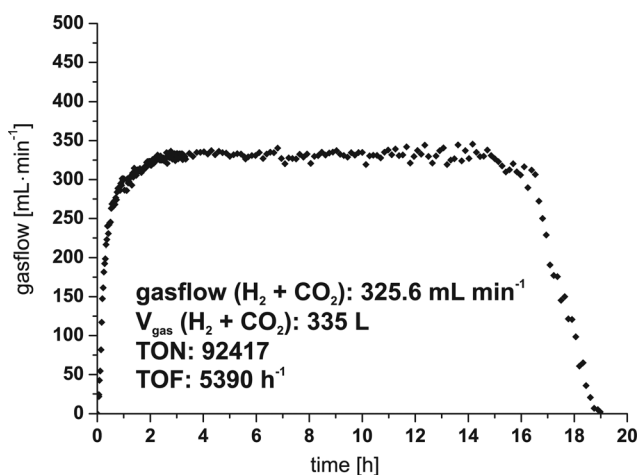


Fig. 3 Continuous formic acid decomposition at $80\ ^\circ C$ over homogeneous $Fe(BF_4)_2 \cdot 6H_2O$ in propylene carbonate. Reproduced from ref. 51 with permission. Copyright AAAS 2011.

production experiment at $80\ ^\circ C$, a stable catalyst activity of $5390\ h^{-1}$ was observed over a period of 16 h. CO concentrations did not exceed 20 ppm.

Based on high pressure *in situ* ^{13}C and ^{31}P NMR spectroscopy and density functional theory calculations the authors propose a reaction mechanism with two competing catalyst cycles with $[FeH(PP_3)]^+$ as the common starting complex. It is interesting to note that under isochoric reaction conditions, *i.e.* an increase of reaction pressure and dissolved product concentration with reaction time and formic acid conversion, a significant change in the catalyst activity is observed. Variation of H_2 and CO_2 partial pressure showed a strong sensitivity of the catalyst activity specifically to the H_2 partial pressure: changing the initial hydrogen pressure from 0 to a moderate 2 MPa resulted in a drop of the TON by $\sim 60\%$. In contrast, the CO_2 pressure did not have any influence on the catalytic activity.

Formic acid decomposition using heterogeneous catalysts

The decomposition of formic acid in the presence of a heterogeneous catalyst is a well-established research subject dating back to the 1930s. However, none of the early work focused on the optimization of hydrogen production, so reaction temperatures were generally high ($>100\ ^\circ C$) and CO formation was rarely measured in detail. Enthaler *et al.* reported a very informative summary of these early research efforts in their excellent review.⁴ In recent years, the rising interest in formic acid as a hydrogen storage material resulted in an increasing amount of dedicated research. Various catalyst screenings of mono- and bimetallic systems have been reported, focusing on low-temperature activity and H_2 selectivity – the main factors in competition with homogeneous systems (Table 2).

Generally however, reaction temperatures are still considerably higher and elevated CO concentrations are observed. Direct decarbonylation of FA and the catalysts' activity for the reverse water gas shift (rWGS) reaction (see Scheme 1) at these temperatures are generally suggested as CO sources.

Recent studies of monometallic noble metal nanoparticles on various support materials yielded some promising catalytic systems. However, the selectivity under (water-free) decomposition conditions is generally not sufficient for fuel cell applications and temperatures close to or above $100\ ^\circ C$ are required to achieve the relevant catalytic activities. Ojeda and Iglesia⁵² recently reported that finely dispersed gold nanoparticles supported on Al_2O_3 , unlike bulk metallic gold,⁵³ can exhibit considerable FA decomposition activity, producing virtually CO-free hydrogen. They conclude that the active metal sites are not situated on TEM-visible metal particles but rather on much smaller Au domains (*e.g.* isolated Au atoms). These findings were in part confirmed by Ross *et al.* in a detailed study of gas phase FA decomposition over commercial Pd/C, Au/TiO₂ and Au/C at various metal loadings.⁵⁴ All catalysts showed promising activity (TOF of $255\ h^{-1}$ for 1% Pd/C at 373 K), but here considerable amounts of CO were observed under all reaction conditions. Solymosi and co-workers investigated the decomposition of FA over a range of monometallic noble metal catalysts (Ir, Pd, Pt, Ru and Rh) supported on high specific surface area (SSA) activated carbon (AC) at elevated temperatures (350–750 K).⁵⁵ Only the Ir based systems yielded high activity at 373 K and high H_2

Table 2 Heterogeneous catalysts for the decomposition of formic acid

Active phase/support	Solvent/medium	Performance	Temp.	Ref.
0.61% Au/Al ₂ O ₃	He/gas phase	TOF = 25 600 h ⁻¹ , ~10 ppm CO	353 K	52
20 wt% PdAu/C–CeO ₂	Aqueous	TOF = 832 h ⁻¹ , <140 ppm CO	375 K	58
1% Pd/C	He/gas phase	TOF = 255 h ⁻¹ , S _{H2} ≈ 99%	373 K	54
Mo ₂ C/C	Ar/gas phase	TOF = 437 h ⁻¹ , S _{H2} = 95–98%	423 K	68
PdAu@Au/C (core–shell)	Aqueous	30 ppm CO	356 K	64
5% Au/CeO ₂	Ar/gas phase	TOF = 295 h ⁻¹ , S _{H2} = 100% ^a	473 K	56
Ir/C	Ar/gas phase	TOF = 960 h ⁻¹ , S _{H2} ≈ 99%	373 K	55
Ag@Pd/C (core–shell)	Aqueous	TOF = 125 h ⁻¹ , S _{H2} = 100%	293 K	65
		TOF = 626 h ⁻¹ , 84 ppm CO	363 K	
Pd–S–SiO ₂	Aqueous	TOF = 803 h ⁻¹ , S _{H2} = 100%	358 K	67

^a Incomplete FA conversion.

selectivity (>99%), while notably, the activity and selectivity over Pd was poor. Again, only the addition of water and a considerable temperature increase (473 K) suppressed CO formation over Ir to the levels appropriate for fuel cell applications. A later study by the same group investigating 1% Au on different support materials (SiO₂, CeO₂ and AC) did not show any fundamentally different catalytic performance than the noble metal systems studied earlier.⁵⁶ Even higher temperatures (>500 K) were needed to reach full FA conversion, leading to the formation of considerable amounts of CO. In a mechanistic study of a Pd(111) catalyst, Vohs and Jeroro⁵⁷ observed a substantial promoting effect of Zn oxide on the FA dehydrogenation selectivity. Unfortunately, no indication of its behavior under realistic reaction conditions is given.

The addition of a secondary metal is a well-known means to alter, amongst other things, the electronic properties of the active phase, its adsorption behavior and the metal dispersion/particle size. Xing and co-workers showed that the introduction of certain copper group metals has a marked effect on the stability of highly dispersed Pd-nanoparticles in aqueous media.⁵⁸ While Pd/C quickly deactivated, Pd–Au/C and Pd–Ag/C with particle sizes of ~3.5 nm (Pd–Au) and 8 nm (Pd–Ag) produced lower CO contamination (a maximum of 80 ppm CO) at a moderate temperature of 92 °C. The equally moderate activity (initial TOF of 27 h⁻¹ for Pd–Au/C) increased dramatically when CeO₂ was introduced as the catalyst promoter.

A maximum TOF of 227 h⁻¹ was reported at 92 °C, increasing to 832 h⁻¹ at 102 °C, for the Pd–Au/C–CeO₂ system (10 wt% Pd, 50 wt% CeO₂, n_{Pd} : n_{Au} = 1 : 1). This increase in activity was assigned to a change in the electronic properties of the active Pd alloy phase. The metal dispersion was found to be affected, but not a key factor for activity. During a continuous stability test, the Pd–Ag catalyst without the CeO₂ promoter showed no signs of deactivation over a period of 240 h on stream. The role of CeO₂ in the decomposition of formic acid had previously been investigated by other researchers.^{59,60} In a follow up study, Xing *et al.* reported a marked effect of rare earth promoters on the activity of their Pd–Au/C catalyst systems (Fig. 4).⁶¹ Recently, Xu and co-workers studied the performance of a number of mono- and bimetallic nanoparticles immobilized inside metal organic frameworks (MOFs) as FA decomposition catalysts.⁶² Of all the catalysts tested, only Au–Pd/MOF (20.4 wt% metal loading, Au : Pd = 2.46) showed promising FA decomposition activity at moderate reaction temperatures (average TOF of

125 h⁻¹ at 90 °C). The catalyst is stable over four reaction cycles, but no detailed measurements of low level CO were done.

An interesting trimetallic system consisting of Pt, Ru and Bi oxide was investigated by Chan *et al.*⁶³ The Bi-oxide does not act as catalyst support, but is co-impregnated on an activated carbon carrier. This system already showed some FA decomposition activity at ambient temperature and showed a reported TOF of 312 h⁻¹ at 80 °C (based on Pt and Ru surface atoms) in aqueous solution, without the formation of CO. Interestingly, Pt–Ru without the Bi oxide did not show any activity for FA dehydrogenation even at high temperatures.

As an alternative to metal alloys, the promotion of the active phase in a core–shell type particle geometry is a fairly new technology. In an initial study, PdAu@Au core–shell nanoparticles supported on activated carbon were tested in the liquid phase decomposition of formic acid (Fig. 5).⁶⁴

Both the activity and stability improved considerably compared to the monometallic Au/C and Pd/C catalysts tested in the same study. Unfortunately, no specific activity data is given. A continuous stability test at the same temperature showed no deactivation of the core–shell catalyst and a stable CO content of 34 ppm after 30 h on stream. Very recently, Tsang and co-workers reported a systematic study of M–Pd

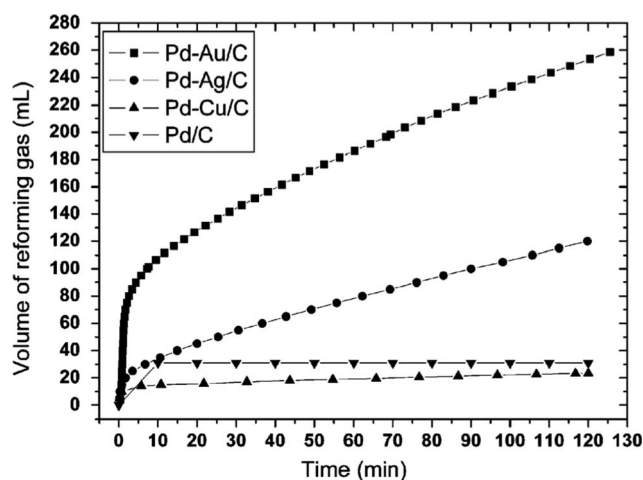


Fig. 4 Formic acid decomposition over different heterogeneous Pd alloy catalysts on a carbon support – effect of CeO₂ promotion. Reproduced from ref. 58 with permission. Copyright The Royal Society of Chemistry 2008.

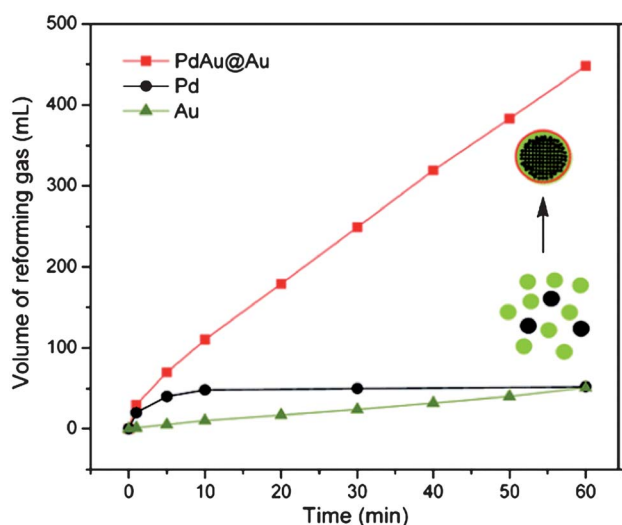


Fig. 5 Formic acid decomposition over heterogeneous Pd–Au catalysts – Synergetic effect of a core–shell particle geometry as compared to monometallic catalysts. Reproduced from ref. 64 with permission. Copyright American Chemical Society 2010.

core–shell nanoparticles ($M = \text{Ru}, \text{Rh}, \text{Pt}, \text{Ag}, \text{Au}$) comparing their performance to monometallic colloidal nanoparticles in D_2O . The high activity of monometallic Pd as an FA decomposition catalyst was confirmed and correlated with the intrinsic electronic properties of the metallic particles. Modifying the electronic properties of the Pd surface by introducing a secondary metal proved most successful for Ag–Pd (1 : 1) core–shell nanoparticles. As compared to monometallic Pd, the TOF increased almost 6-fold at 293 K (125 h^{-1}) to a maximum of 626 h^{-1} at 363 K.⁶⁵ Only at high temperatures was a moderate CO concentration of 84 ppm observed. After immobilization on high SSA AC and surfactant removal, the resulting Ag@Pd/C catalyst showed a further increase in the FA decomposition activity (196 h^{-1} at 293 K) without any deterioration of the H_2 selectivity.

As opposed to deposited metal nanoparticles, the immobilization of high performance homogeneous catalysts holds the promise of an easy way to combine excellent catalytic performance at low temperatures with the improved catalyst handling and reusability of heterogeneous systems. In our group, efforts in this direction were made to immobilize our highly active Ru-*m*TPPTS catalyst³³ via ion exchange, polymer immobilization and physical adsorption on various supports.⁶⁶ High initial activity was observed in all cases, followed by severe deactivation. Recently, Guo and co-workers investigated the decomposition of formic acid over single-atom Pd and Ru on functionalized SiO_2 supports in an aqueous HCOOH – HCOONa solution.⁶⁷ A mercapto-functionalized Pd–S– SiO_2 gave a stable TOF of 803 h^{-1} at 85°C after multiple catalyst recycles. It is interesting to note that support functionalisation with PPh_3 or TPPTS, both common ligands in high performance homogeneous systems, resulted in only mediocre catalytic performance.

The only competitive alternative to noble metal catalysts, *i.e.* with similar activity and H_2 selectivity so far remains molybdenum carbide. Solymosi and co-workers investigated Mo_2C

supported on carbon nanotubes (CNT) and high SSA AC at reaction temperatures between 350 and 750 K for both the decomposition and steam reforming of FA.⁶⁸ The most promising catalytic performance was observed for the AC-supported catalysts. 1% Mo_2C on AC gave full FA conversion at 423 K (TOF of 437 h^{-1} , based on bulk Mo_2C as the active phase), with H_2 selectivities between 95 and 98%. Similar to the noble metal systems investigated by the same group, the addition of water effectively suppressed the formation of CO over this catalyst, probably due to a shift in the WGS equilibrium towards H_2/CO_2 . Interestingly, the same active phase supported on SiO_2 gave low decomposition activity and H_2 selectivity ($<70\%$). A mechanistic study of FA decomposition on unsupported Mo(110) and C-Mo(110) surfaces⁶⁹ observed an increase of H_2 selectivity by as much as 1500% in the presence of carbidic carbon. This effect is assigned to the blocking of active sites responsible for FA dehydration and a decreased activation energy for direct gas-phase dehydrogenation. Recently, a Cu_2O photocatalyst was shown to selectively decompose an aqueous formic acid solution into CO_2/H_2 in the presence of visible light.⁷⁰

Several metal oxides (TiO_2 , V_2O_3 , Cr_2O_3 , MnO) have been known to be active FA decomposition catalysts.⁷¹ Recent studies include V–Ti–O⁷² as well as the photocatalytic decomposition over Fe^{II} (photo-Fenton reaction with H_2O_2),^{73,74} pure TiO_2 in water^{75–77} and in the gas phase,⁷⁸ as well as alkaline earth titanates in water.⁷⁹ However, these studies are primarily concerned with the removal of dilute formic acid from wastewater or off-gas streams, and H_2 selectivities are generally low or not investigated at all.

An interesting, albeit less studied, alternative to the thermal decomposition of FA over heterogeneous catalysts is the electrochemical H_2 generation by FA electrolysis at electrocatalysts. The process was first studied by Aldous and Compton, using different Pt and Pt/carbon electrode arrangements in aqueous FA solutions and a eutectic mixture of FA and $[\text{NH}_4][\text{HCOO}]$.⁸⁰ Only the latter approach led to the successful electrolysis of formic acid and the production of hydrogen. Later, the successful electrolysis of FA in aqueous NaOH solution was reported, using bulk Pt foil electrodes.⁸¹ However, current densities were still low ($<8 \text{ mA cm}^{-2}$). This year Coutanceau and co-workers investigated the effect of catalyst composition on the performance of a proton exchange membrane electrolysis cell in the decomposition of FA.⁸² Several Pd/Au and Pd/Pt alloys of varying composition supported on carbon were tested and compared to a basic Pd/C catalyst. While the Pt free catalyst showed promising initial activity and overpotential (100 mA cm^{-2} and $0.2\text{--}0.4 \text{ V}$ resp.), it proved susceptible to CO poisoning and deactivation. In general it has to be said that this approach suffers from a number of inherent drawbacks that cannot be overcome by a breakthrough in catalyst research. For one, replacing heat with an electrical potential as the driving force seems much less favorable energetically, considering that low- or no-value heat ($50\text{--}140^\circ\text{C}$) is replaced by pure energy with its own long line of losses on its way to the electrolysis cell. Also, even though the electrolysis of FA might be more efficient than that of water – a fact pointed out in all the studies discussed above – the latter is considered a viable source of H_2 only because of the general availability.

Technological approaches and challenges

In 2010, Enthaler and co-workers stated that comparing the FA based fuel cell power of ~ 47 mW achieved by Beller and co-workers “to the energy demand of an incandescent lamp (60 W), the long distance is apparent for reaching a general application” of formic acid based energy sources.⁴ As a similar proof of principle experiment based on a heterogeneous catalyst⁶¹ marks the state of application-related research today, this evaluation of the state of research in general still holds true. With the exception of the control concept developed by Majewski *et al.*,⁴⁰ research activities are still fully focused on catalyst optimization on the level of active phase composition. This almost total absence of engineering research is even more baffling when the general claim of FA as an ideal fuel for compact mobile applications is put up against pressing questions such as accumulation of residual water, solvent entrainment in the product gas, optimization of catalyst bed structure or an efficient reactor heating concept. To identify the main technological obstacles on the way to an efficient use of FA as a hydrogen source and storage material, a hydrogen generator based on the decomposition of FA over a homogeneous Ru(II) catalyst was designed and built in our lab. While the general concept was published earlier,⁸³ the project is still a work in progress, so detailed results will be published at a later date. The hydrogen generator successfully met the target power output of 1 kW_{el} or roughly 30 L min⁻¹ of H₂/CO₂ assuming 50% fuel cell efficiency (Fig. 6).

The product flow rate is controlled using a standard mass flow controller, while the reaction pressure is maintained by a controlled formic acid feed flow. The free reactor volume is used as a buffer in case of rapid changes in the product flow rate set point. Therefore the system was designed around a 5 L reaction vessel with electrical surface heating elements, containing 11.8 g of RuCl₃·3H₂O (0.045 mole) and 51.2 g Na₃TPPTS (0.090 mole) catalyst in 1.5 L aqueous HCOONa solution (1 M). The resulting free reactor volume also serves for gas–liquid separation and effectively prevents foam or spray from reaching the product gas outlet. To minimize water vapour entrainment in the product gas, the system also comprises a product gas cooler with condensate separator/recycle. As the control concept does not comprise the measurement of pH or formic acid concentration in the catalyst solution, the reaction has to run at a large catalyst excess for reasons of process safety. This setup has been used safely for over one year without the need to exchange or replenish the catalyst solution.

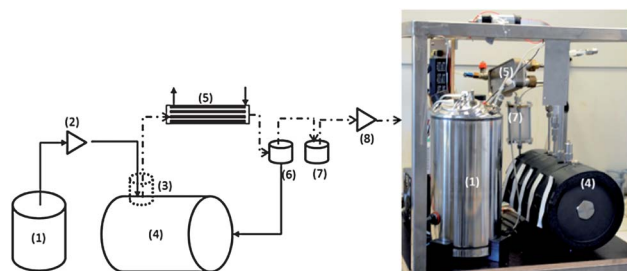


Fig. 6 A hydrogen generator designed and built in our laboratories for a power output of 1 kW_{el} (30 L min⁻¹ of H₂/CO₂) (1) Formic acid tank; (2) pump; (3) tube in tube heat exchanger; (4) reactor; (5) heat exchanger; (6 and 7) condensate separators; (8) mass flow controller.

Concerning the use of heterogeneous catalysts for the decomposition of FA, it is clear that the development of a suitable heterogeneous catalyst bed with optimized heat and mass transfer characteristics, taking into account the particular multiphase flow pattern and the slightly endothermic nature of the process will require further research. However, an approach from the technological and engineering side raises a different quite fundamental question: we feel that a clear justification for the use of heterogeneous catalytic systems in FA based hydrogen generation – at least in the way it has been approached so far – has been strangely neglected. Usually, heterogeneous catalysts are employed in processes where catalyst separation from the (liquid) product mixture is a prerequisite for its reuse and/or where harsh reaction conditions rule out less robust homogeneous alternatives. On close inspection, none of these factors apply to the decomposition of formic acid. In fact, its main advantage over other liquid hydrogen carriers is specifically the high hydrogen production rates at near ambient temperature, while the catalyst/product gas separation is particularly easy. On the other hand, multi-phase systems using heterogeneous catalysts are notorious for their complex heat and mass transfer requirements, putting a whole new set of development issues on the table. In view of these considerations the use of heterogeneous catalysts can only be justified where diluted FA is used as the feedstock and the solvent needs to be continuously evacuated from the reactor. However, this constraint with its impact on experimental conditions has not necessarily found its way into today’s catalyst research.

Conclusions

It has been some time now since formic acid was identified as one of the most promising materials for hydrogen storage. It can even be considered a superior alternative to methanol, since under ambient conditions it is a liquid with low toxicity, having a flash point well above room temperature and a hydrogen content of 4.4 wt%. Furthermore, the simplicity and elegance of the combination of formic acid and H₂/CO₂ as a reversible hydrogen storage system certainly sounds appealing, since the hydrogenation of CO₂/HCO₃⁻ over homogeneous catalysts has been achieved with excellent activities. Recent advances in catalyst development have opened up the opportunity to fully exploit these advantages using either homogeneous or heterogeneous catalysts: there are today a number of highly active and robust homogeneous catalysts described and investigated in the literature that selectively decompose formic acid to H₂ and CO₂ close to room temperature.

Concerning heterogeneous FA decomposition catalysts, the situation is similar to homogeneous systems. While the activity and H₂ selectivity have not yet reached the level of homogeneous systems, and most heterogeneous systems investigated still suffer from a more or less pronounced decarbonylation activity, this gap is closing. In particular, the recent application of state-of-the-art nanoparticle synthesis methods has led to a range of high performance catalysts such as core–shell combinations of Pd and Au, yielding high quality H₂ with low CO content.

A first successful hydrogen production from FA on the scale of 1 kW_{el} was realized in our lab. However, this attempt also demonstrates the large potential for optimization entailed in

reactor scale up. To take only two examples, electrical heating and water cooled condensate traps are fine solutions for stationary lab applications but different/autonomous solutions have to be used for mobile applications in the “real world”, e.g. catalytic H₂ or FA combustion as the heat source and a radiator-type gas cooler.

Acknowledgements

The Swiss National Science Foundation and EPFL are thanked for financial support.

Notes and references

- J. O. M. Bockris, *Science*, 1972, **176**, 1323.
- R. von Helmolt and U. Eberle, *J. Power Sources*, 2007, **165**, 833–843.
- M. Felderhoff, C. Weidenthaler, R. von Helmolt and U. Eberle, *Phys. Chem. Chem. Phys.*, 2007, **9**, 2643–2653.
- S. Enthaler, J. von Langermann and T. Schmidt, *Energy Environ. Sci.*, 2010, **3**, 1207–1217.
- H.-L. Jiang, S. K. Singh, J.-M. Yan, X.-B. Zhang and Q. Xu, *ChemSusChem*, 2010, **3**, 541–549.
- T. C. Johnson, D. J. Morris and M. Wills, *Chem. Soc. Rev.*, 2010, **39**, 81–88.
- B. Loges, A. Boddien, F. Gaertner, H. Junge and M. Beller, *Top. Catal.*, 2010, **53**, 902–914.
- P. Makowski, A. Thomas, P. Kuhn and F. Goettmann, *Energy Environ. Sci.*, 2009, **2**, 480–490.
- W. K. Reutemann and H. Kieczka, *Ullmann's Encyclopedia of Industrial Chemistry*, Wiley-VCH, Weinheim, 2011.
- R. Xing, W. Qi and G. W. Huber, *Energy Environ. Sci.*, 2011, **4**, 2193–2205.
- F. Jin and H. Enomoto, *Energy Environ. Sci.*, 2011, **4**, 382–397.
- D. J. Fitzpatrick, S. Hayes, M. H. B. Hayes and J. R. H. Ross, *Biorefineries – Industrial Processes and Products*, ed. B. G. Kamm, P. R. Gruber and M. Kamm, Wiley-VCH, Weinheim, 2010, ch. 7, p. 139.
- G. Centi and S. Perathoner, *Catal. Today*, 2009, **148**, 191–205.
- Office of Energy Efficiency and Renewable Energy; The FreedomCAR and Fuel Partnership, *Targets For Onboard Hydrogen Storage Systems For Light-duty Vehicles*, September 2009, <http://www1.eere.energy.gov>.
- U. B. Demirci and P. Miele, *Energy Environ. Sci.*, 2011, **4**, 3334–3341.
- N. V. Rees and R. G. Compton, *J. Solid State Electrochem.*, 2011, **15**, 2095–2100.
- P. G. Jessop, *The Handbook of Homogeneous Hydrogenation*, Wiley-VCH Verlag GmbH, Weinheim, 2008, pp. 489–511.
- S. Enthaler, *ChemSusChem*, 2008, **1**, 801–804.
- F. Joo, *ChemSusChem*, 2008, **1**, 805–808.
- G. A. Olah, G. K. S. Prakash and A. Goepfert, *J. Am. Chem. Soc.*, 2011, **133**, 12881–12898.
- R. S. Coffey, *Chem. Commun.*, 1967, 923.
- T. Yoshida, T. Yamagata, T. H. Tulip, J. A. Ibers and S. Otsuka, *J. Am. Chem. Soc.*, 1978, **100**, 2063–2073.
- S. H. Strauss, K. H. Whitmire and D. F. Shriver, *J. Organomet. Chem.*, 1979, **174**, C59–C62.
- R. S. Paonessa and W. C. Troglor, *J. Am. Chem. Soc.*, 1982, **104**, 3529–3530.
- Y. Gao, J. K. Kuncheria, H. A. Jenkins, R. J. Puddephatt and G. P. A. Yap, *J. Chem. Soc., Dalton Trans.*, 2000, 3212–3217.
- Y. Himeda, N. Onozawa-Komatsuzaki, H. Sugihara, H. Arakawa and K. Kasuga, *Organometallics*, 2004, **23**, 1480–1483.
- S. Fukuzumi, T. Kobayashi and T. Suenobu, *ChemSusChem*, 2008, **1**, 827–834.
- A. Boddien, B. Loges, H. Junge and M. Beller, *ChemSusChem*, 2008, **1**, 751–758.
- H. Junge, A. Boddien, F. Capitta, B. Loges, J. R. Noyes, S. Gladiali and M. Beller, *Tetrahedron Lett.*, 2009, **50**, 1603–1606.
- A. Boddien, B. Loges, H. Junge, F. Gaertner, J. R. Noyes and M. Beller, *Adv. Synth. Catal.*, 2009, **351**, 2517–2520.
- B. Loges, A. Boddien, H. Junge and M. Beller, *Angew. Chem., Int. Ed.*, 2008, **47**, 3962–3965.
- B. Loges, A. Boddien, H. Junge, J. R. Noyes, W. Baumann and M. Beller, *Chem. Commun.*, 2009, 4185–4187.
- C. Fellay, P. J. Dyson and G. Laurenczy, *Angew. Chem., Int. Ed.*, 2008, **47**, 3966–3968.
- C. Fellay, N. Yan, P. J. Dyson and G. Laurenczy, *Chem.–Eur. J.*, 2009, **15**, 3752–3760.
- W. Gan, C. Fellay, P. J. Dyson and G. Laurenczy, *J. Coord. Chem.*, 2010, **63**, 2685–2694.
- S. Fukuzumi, T. Kobayashi and T. Suenobu, *J. Am. Chem. Soc.*, 2010, **132**, 1496–1497.
- Y. Himeda, *Eur. J. Inorg. Chem.*, 2007, 3927–3941.
- Y. Himeda, *Green Chem.*, 2009, **11**, 2018–2022.
- D. J. Morris, G. J. Clarkson and M. Wills, *Organometallics*, 2009, **28**, 4133–4140.
- A. Majewski, D. J. Morris, K. Kendall and M. Wills, *ChemSusChem*, 2010, **3**, 431–434.
- M. Czaun, A. Goepfert, R. May, R. Haiges, G. K. S. Prakash and G. A. Olah, *ChemSusChem*, 2011, **4**, 1241–1248.
- X. Li, X. Ma, F. Shi and Y. Deng, *ChemSusChem*, 2010, **3**, 71–74.
- J. D. Scholten, M. H. G. Prechtel and J. Dupont, *ChemCatChem*, 2010, **2**, 1265–1270.
- Y. Yasaka, C. Wakai, N. Matubayasi and M. Nakahara, *J. Phys. Chem. A*, 2010, **114**, 3510–3515.
- M. E. M. Berger, D. Assenbaum, N. Taccardi, E. Spiecker and P. Wasserscheid, *Green Chem.*, 2011, **13**, 1411–1415.
- A. Boddien, F. Gaertner, C. Federsel, P. Sponholz, D. Mellmann, R. Jackstell, H. Junge and M. Beller, *Angew. Chem., Int. Ed.*, 2011, **50**, 6411–6414.
- C. Federsel, R. Jackstell, A. Boddien, G. Laurenczy and M. Beller, *ChemSusChem*, 2010, **3**, 1048–1050.
- G. Papp, J. Csorba, G. Laurenczy and F. Joó, *Angew. Chem., Int. Ed.*, 2011, **50**, 10433–10435.
- A. Boddien, B. Loges, F. Gaertner, C. Torborg, K. Fumino, H. Junge, R. Ludwig and M. Beller, *J. Am. Chem. Soc.*, 2010, **132**, 8924–8934.
- A. Boddien, F. Gaertner, R. Jackstell, H. Junge, A. Spannenberg, W. Baumann, R. Ludwig and M. Beller, *Angew. Chem., Int. Ed.*, 2010, **49**, 8993–8996.
- A. Boddien, D. Mellmann, F. Gaertner, R. Jackstell, H. Junge, P. J. Dyson, G. Laurenczy, R. Ludwig and M. Beller, *Science*, 2011, **333**, 1733–1736.
- M. Ojeda and E. Iglesia, *Angew. Chem., Int. Ed.*, 2009, **48**, 4800–4803.
- J. Fahrenfort, L. L. Vanreijen and W. M. H. Sachtler, *Z. Elektrochem.*, 1960, **64**, 216–224.
- D. A. Bulushev, S. Beloshapkin and J. R. H. Ross, *Catal. Today*, 2010, **154**, 7–12.
- F. Solymosi, A. Koos, N. Liliom and I. Ugrai, *J. Catal.*, 2011, **279**, 213–219.
- A. Gazsi, T. Bansagi and F. Solymosi, *J. Phys. Chem. C*, 2011, **115**, 15459–15466.
- E. Jeroro and J. M. Vohs, *Catal. Lett.*, 2009, **130**, 271–277.
- X. Zhou, Y. Huang, W. Xing, C. Liu, J. Liao and T. Lu, *Chem. Commun.*, 2008, 3540–3542.
- S. D. Senanayake and D. R. Mullins, *J. Phys. Chem. C*, 2008, **112**, 9744–9752.
- Y. Xu, W. O. Gordon, S. D. Senanayake, D. R. Mullins and S. H. Overbury, *Abstr. Pap. Am. Chem. Soc.*, 2009, 237.
- X. Zhou, Y. Huang, C. Liu, J. Liao, T. Lu and W. Xing, *ChemSusChem*, 2010, **3**, 1379–1382.
- X. Gu, Z.-H. Lu, H.-L. Jiang, T. Akita and Q. Xu, *J. Am. Chem. Soc.*, 2011, **133**, 11822–11825.
- S.-W. Ting, S. Cheng, K.-Y. Tsang, N. van der Laak and K.-Y. Chan, *Chem. Commun.*, 2009, 7333–7335.
- Y. Huang, X. Zhou, M. Yin, C. Liu and W. Xing, *Chem. Mater.*, 2010, **22**, 5122–5128.
- K. Tedsree and T. Li, *Nat. Nanotechnol.*, 2011, **6**, 302–307.
- W. Gan, P. J. Dyson and G. Laurenczy, *React. Kinet. Catal. Lett.*, 2009, **98**, 205–213.
- Y. Zhao, L. Deng, S.-Y. Tang, D.-M. Lai, B. Liao, Y. Fu and Q.-X. Guo, *Energy Fuels*, 2011, **25**, 3693–3697.
- A. Koos and F. Solymosi, *Catal. Lett.*, 2010, **138**, 23–27.
- D. W. Flaherty, S. P. Berglund and C. B. Mullins, *J. Catal.*, 2010, **269**, 33–43.
- S. Kakuta and T. Abe, *ACS Appl. Mater. Interfaces*, 2009, **1**, 2707–2710.

- 71 J. M. Criado, F. Gonzalez and J. M. Trillo, *J. Catal.*, 1971, **23**, 11–18.
- 72 E. A. Ivanov, G. Y. Popova, Y. A. Chesalov and T. V. Andrushkevich, *J. Mol. Catal. A: Chem.*, 2009, **312**, 92–96.
- 73 J. Farias, E. D. Albizzati and O. M. Alfano, *Catal. Today*, 2009, **144**, 117–123.
- 74 J. Farias, G. H. Rossetti, E. D. Albizzati and O. M. Alfano, *Ind. Eng. Chem. Res.*, 2007, **46**, 7580–7586.
- 75 G. R. Dey, K. N. R. Nair and K. K. Pushpa, *J. Nat. Gas Chem.*, 2009, **18**, 50–54.
- 76 H. J. Yun, H. Lee, J. B. Joo, W. Kim and J. Yi, *J. Phys. Chem. C*, 2009, **113**, 3050–3055.
- 77 Y. Iwasawa, *Abstr. Pap. Am. Chem. Soc.*, 2007, 233.
- 78 K. L. Miller, C. W. Lee, J. L. Falconer and J. W. Medlin, *J. Catal.*, 2010, **275**, 294–299.
- 79 B. Zielinska, E. Borowiak-Palen and R. J. Kalenczuk, *Int. J. Hydrogen Energy*, 2008, **33**, 1797–1802.
- 80 L. Aldous and R. G. Compton, *Energy Environ. Sci.*, 2010, **3**, 1587–1592.
- 81 W. L. Guo, L. Li, L. L. Li, S. Tian, S. L. Liu and Y. P. Wu, *Int. J. Hydrogen Energy*, 2011, **36**, 9415–9419.
- 82 C. Lamy, A. Devadas, M. Simoes and C. Coutanceau, *Electrochim. Acta*, 2012, **60**, 112–120.
- 83 G. G. Laurency, M. Grasmann, B. Lorent and P. Raspail, *Electrosuisse Bull.*, 2011, **7**, 33–37.
- 84 Y. Himeda, S. Miyazawa and T. Hirose, *ChemSusChem*, 2011, **4**, 487–493.